SOURCE: *Signal Processing and Speech Communication Lab, Graz University of Technology, Austria

**Communication Technology Laboratory, Swiss Federal Institute of Technology Zurich, Switzerland

†Institute of Communications and Radio-Frequency Engineering, Vienna University of Technology, Austria

SAGE Algorithm for UWB Channel Parameter Estimation

Katharina Hausmair*, Klaus Witrisal*, Paul Meissner*,
Christoph Steiner**, Georg Kail†
Contact: Katharina Hausmair, Klaus Witrisal
Graz University of Technology
Inffeldgasse 12
A-8010 Graz
Austria
Phone: +43 316 873 4431
Fax: +43 316 873 4432
Email: hausmair@sbox.tugraz.at, witrisal@tugraz.at

SAGE Algorithm for UWB Channel Parameter Estimation

Katharina Hausmair*, Klaus Witrisal*, Paul Meissner*,
Christoph Steiner** and Georg Kail†
*Signal Processing and Speech Communication Laboratory, Graz University of Technology, Austria,
Email: hausmair@sbox.tugraz.at, {witrisal, paul.meissner}@tugraz.at
**Communication Technology Laboratory, Swiss Federal Institute of Technology Zurich, Switzerland,
Email: steinech@nari.ee.ethz.ch
†Institute of Communications and Radio-Frequency Engineering, Vienna University of Technology, Austria,
Email: gkail@nt.tuwien.ac.at

Abstract— **UWB signals have become popular for ranging and positioning systems. Since such systems require the extraction of location related information from the radio channel, efficient methods are required to obtain the parameters of interest. This paper presents a simple extension to the SAGE algorithm that makes the algorithm suitable for analyzing UWB channels. It is demonstrated that a phased array beamformer in combination with time gating eliminates the need for more complex delay-and-sum beamforming in the maximization step. The performance of the proposed procedure is demonstrated by applying the algorithm to measurement data.**

I. INTRODUCTION

Due to the advantages provided by the use of large bandwidths, UWB systems offer a great range of possibilities for a variety of applications. For communication systems high data rate transmission and robustness against fading, as well as the ability to coexist with other systems are of huge interest. The excellent temporal resolution that is achieved by the use of large bandwidths in UWB systems enables the design of accurate ranging and positioning systems. Such systems require the extraction of location related information like angles of arrival and delays of multipath components (MPCs) from the radio channel [1]. Hence, efficient methods are required to extract the parameters of interest from channel measurement data.

For that purpose, a number of different algorithms have been proposed. Algorithms using successive cancellation techniques like the Sensor-CLEAN algorithm [2] and extensions [3] assume the received signal to be a sum of pulses. Channel parameters are estimated by searching for the largest pulse in the received signal, subtracting the contribution of the found pulse from the signal, and then repeating the procedure until the energy of the largest found pulse falls below a certain threshold. Quite similar to these algorithms, the SAGE algorithm, which was originally developed for narrowband systems, has recently been proposed to estimate UWB channel parameters in the frequency domain in [4] and [5].

In this paper the SAGE algorithm, which is applied in [6] for time domain channel parameter estimation in wideband systems, is extended to achieve high accuracy in both azimuth and delay estimation of MPCs in UWB channels. The proposed algorithm relies on narrowband beamforming in combination with time gating, which eliminates the need for more complex delay-and-sum beamforming, and a matched filter. Our approach is based on array measurements and, similar to the Sensor-CLEAN, assumes the received signal to be the sum of pulses reaching the receiver at different delays from distinct angles.

The paper is organized as follows. Section II defines the underlying signal model. In Section III the SAGE algorithm is explained, while Section IV describes the necessary extension for UWB channel parameter estimation. The performance of the proposed estimation procedure is presented in Section V by applying the algorithm to measurement data.

II. SIGNAL MODEL

The signal model is based on existing models for parameter estimation using the EM or SAGE algorithm with wideband signals, as can be found in [6]–[9]. Instead of transmitting a periodically repeated burst signal that consists of a wideband shaping pulse modulated by a sounding sequence, the transmitted signal in this model is a single UWB pulse burst. Due to the large bandwidth, excellent time resolution can be achieved in the estimation procedure to resolve the different waves that impinge at the receiver.

A single input multiple output (SIMO) antenna configuration with one transmitter and a measurement array with M equidistant antennas at the receiver serves as transmission scheme. Both transmitter and receiver are considered to remain approximately stationary for the duration of a measurement, and therefore Doppler spread does not have to be considered.

All the described signals are given in their baseband representations, as the following estimation is performed in the baseband.

The transmitted signal $p(t)$ is a single UWB pulse. It is assumed in the propagation model that the received signal $\underline{Y}(t)$ consists of a finite number L of plane waves that are impinging at the receiver antennas. The received signal at the output of the antenna array can be expressed in vector notation as a superposition of these L multipath components corrupted by additive noise as

$$
\begin{aligned}
\underline{Y}(t) &\triangleq [Y_1(t), \ldots, Y_M(t)]^T \\
&= \sum_{l=1}^{L} \underline{s}(t; \underline{\theta}_l) + \sqrt{\frac{N_0}{2}} \underline{N}(t) \\
&= \underline{s}(t; \underline{\theta}) + \sqrt{\frac{N_0}{2}} \underline{N}(t) \quad (1)
\end{aligned}
$$

In this equation the vector $\underline{N}(t) \triangleq [N_1(t), \ldots, N_M(t)]^T$ contains spatially independent complex white Gaussian noise and N_0 is a positive constant, while $\underline{s}(t; \underline{\theta}_l)$ stands for the contribution of the lth MPC to the M received baseband signals. All wave contributions are summed up in $\underline{s}(t; \underline{\theta}) = \sum_{l=1}^{L} \underline{s}(t; \underline{\theta}_l)$, where $\underline{\theta} \triangleq [\underline{\theta}_1, \ldots, \underline{\theta}_L]$ contains the parameters of all the waves.

A single MPC with index l is characterized by its relative delay τ_l, incident azimuth ϕ_l and complex amplitude α_l. These parameters are contained in the vector $\underline{\theta}_l \triangleq [\tau_l, \phi_l, \alpha_l]$. The vector of the contribution of the lth wave to the M received baseband signals is given by

$$
\begin{aligned}
\underline{s}(t; \underline{\theta}_l) &\triangleq [s_1(t; \underline{\theta}_l), \ldots, s_M(t; \underline{\theta}_l)]^T \\
&= \underline{c}(\phi_l) \, \alpha_l \, p(t - \tau_l) \quad (2)
\end{aligned}
$$

where $\underline{c}(\phi_l) \triangleq [c_1(\phi_l), \ldots, c_M(\phi_l)]^T$ is the steering vector of the antenna array. Its components are given by

$$
c_m(\phi) = f_m(\phi) \, e^{j2\pi\lambda^{-1}(\Delta x_m \cos\phi + \Delta y_m \sin\phi)} \quad (3)
$$

with λ denoting the wavelength matching the signal center frequency, $f_m(\phi)$ denoting the complex electric field pattern of the mth antenna, and Δx_m and Δy_m standing for the displacement of the mth antenna in x- and y-directions with respect to an arbitrary reference point.
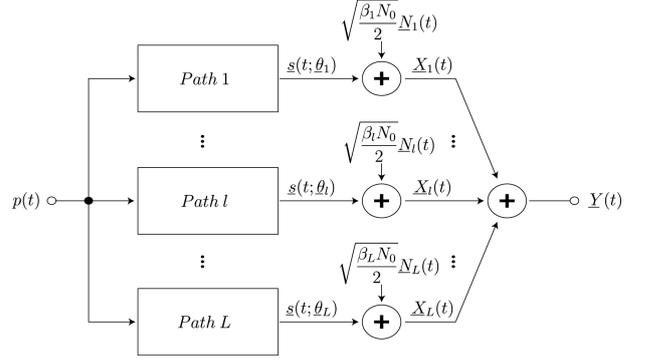

Fig. 1: Relation between complete and incomplete data [8].

III. PARAMETER ESTIMATION USING THE SAGE ALGORITHM

The problem to be solved is the estimation of the parameters that characterize the L deterministic multipath components that impinge at the receiver. The SAGE algorithm [6], [8]–[10] can be applied to solve this problem. For the SAGE procedure the measured received signal $\underline{Y}(t)$ is regarded as the incomplete, but observable data, which is a function of the complete, but unobservable data $\underline{X}(t)$. The individual multipath components, corrupted by a part of the additive noise, are considered as the complete data (see Fig. 1):

$$
\begin{aligned}
\underline{X}_l(t) &\triangleq [X_{l,1}(t), \ldots, X_{l,M}(t)]^T \\
&= \underline{s}(t; \underline{\theta}_l) + \sqrt{\frac{\beta_l N_0}{2}} \underline{N}_l(t) \quad (4)
\end{aligned}
$$

so that

$$
\underline{Y}(t) = \sum_{l=1}^{L} \underline{X}_l(t). \quad (5)
$$

Since the complete data is not actually measurable, it has to be estimated from an observation $\underline{y}(t)$ of the incomplete data and a previous estimate $\hat{\underline{\theta}}'$ of the parameter vector by taking its conditional expectation:

$$
\hat{\underline{x}}_l(t; \hat{\underline{\theta}}') \triangleq E_{\hat{\underline{\theta}}'} \left\{ \underline{X}_l(t) \mid \underline{y}(t) \right\}. \quad (6)
$$

This computation is referred to as the Expectation (E) step of the algorithm. Using (4) the complete data for a single wave can be computed by [7]

$$
\hat{\underline{x}}_l(t; \hat{\underline{\theta}}') = \underline{s}(t; \hat{\underline{\theta}}'_l) + \beta_l \left[\underline{y}(t) - \sum_{l'=1}^{L} \underline{s}(t; \hat{\underline{\theta}}'_{l'}) \right]. \quad (7)
$$

In these equations the first term stands for the contribution of the specific multipath component, and the second term is an estimate of the additive noise, computed by subtracting all wave contributions from the received signal. Since less informative complete data spaces improve
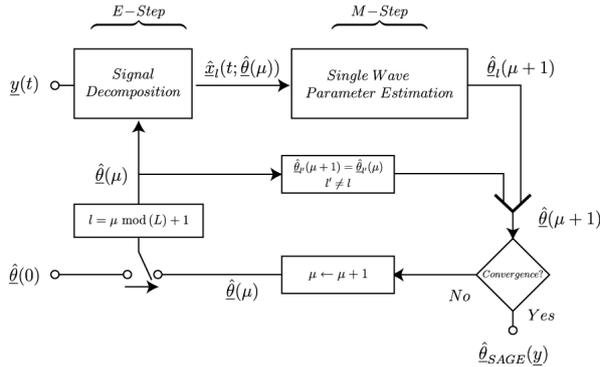
Fig. 2: Signal flow graph of the SAGE algrithm [8].

Fig. 3: Illustration of multiple wave detection problem.

the asymptotic convergence rate of the algorithm [10], β_l is selected to equal 1, as this setting minimizes the information provided by $\underline{X}_l(t)$ about $\underline{\theta}_l$ [9].

In the so called Maximization (M) step of the SAGE algorithm the parameters of one MPC are estimated by finding the maximum likelihood estimate of the log-likelihood function $L(\underline{\theta}_l; \underline{x}_l)$ of the parameter vector of one single wave for an observation $\underline{x}_l(t)$

$$L(\underline{\theta}_l; \underline{x}_l) = \frac{1}{\beta_l N_0} \left(2 \int_T \Re \left\{ \underline{s}^H(t'; \underline{\theta}_l) \underline{x}_l(t') \right\} dt' \right.$$
$$\left. - \int_T \|\underline{s}(t'; \underline{\theta}_l)\|^2 dt' \right) \quad (8)$$

where T is the observation span [8]. For the estimation of all L wave parameters it takes one SAGE cycle, consisting of L iterations (see Fig. 2). As the values of the complex amplitudes α_l can be expressed in closed form as a function of the other parameters, the parameter vector $\hat{\underline{\theta}}_l'' = (\hat{\underline{\theta}}_l)_{ML}(\hat{\underline{x}}_l(t; \hat{\underline{\theta}}'))$ of one wave can be estimated by successively varying τ_l and ϕ_l and then computing α_l [8]:

$$\hat{\tau}_l'' = \arg \max_\tau \left\{ \left| z(\tau, \hat{\phi}_l'; \hat{\underline{x}}_l(t; \hat{\underline{\theta}}')) \right| \right\}$$
$$\hat{\phi}_l'' = \arg \max_\phi \left\{ \left| z(\hat{\tau}_l'', \phi; \hat{\underline{x}}_l(t; \hat{\underline{\theta}}')) \right| \right\}$$
$$\hat{\alpha}_l'' = \frac{z(\hat{\tau}_l'', \hat{\phi}_l''; \hat{\underline{x}}_l(t; \hat{\underline{\theta}}'))}{\left\| \underline{c}(\hat{\phi}_l'') \right\|^2 \int_0^T |p(t - \hat{\tau}_l'')|^2 dt} \quad (9)$$

where

$$z(\tau, \phi; \underline{x}_l) \triangleq \int_0^T p^H(t' - \tau) \, \underline{c}^H(\phi) \, \underline{x}_l(t') \, dt' \quad (10)$$

and $\|\underline{c}(\phi)\|^2 = \sum_{m=1}^M |f_m(\phi)|^2$, which, considering an approximately uniform antenna pattern for all incident angles, equals M. The cost function $z(\tau, \phi; \underline{x}_l)$ can be realized by performing narrowband beamforming to compensate for the phase differences of the signals arriving at different antennas, and then passing the result
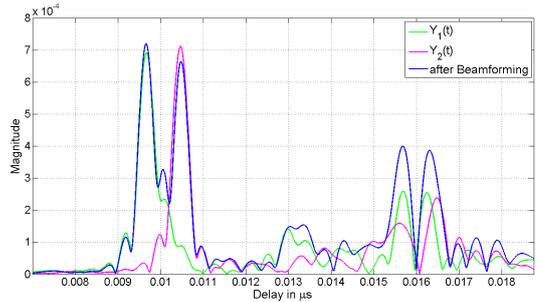
of the beamforming procedure through a filter matched to the transmitted pulse form [7], [8].

E-step and M-step are consecutively executed, generating a sequence of estimates $\{\hat{\underline{\theta}}(\mu)\}$, $\mu = 0, 1, \ldots$, until convergence is achieved.

Note that the SAGE algorithm is designed only to estimate the wave parameters, but not the number of multipath components impinging at the receiver. Therefore, the number of waves L has to be predetermined. The value for L has to be chosen large enough to capture all the dominant waves.

To compute an initial estimate $\underline{\theta}(0)$ all parameters are set to zero and successive interference cancellation is applied [8].

IV. SAGE FOR UWB

Since the UWB sounding pulse provides extremely high time resolution, applying narrowband beamforming can lead to multiple detection of strong waves, and because of that, the SAGE estimation procedure explained in Section III is not an optimal solution for the problem at hand. The reason for multiple wave detection is, that only the differences in the phases of the MPCs arriving at different antenna locations are considered, but not the slight differences in time. For a narrowband signal with low time resolution, this would not cause any problem, but for an UWB signal, the time differences at the antennas can be resolved. Therefore, when correcting the phase differences and then adding up the signals from the M antennas, as done in the beamforming part, more than one maximum for one and the same wave might occur. These maxima can then lead to the repeated detection of that specific wave. An illustration of this problem is shown in Fig. 3. The highest peaks of the signals $Y_1(t)$ and $Y_2(t)$ respectively, measured for a transmitted pulse with 4000MHz bandwidth at center frequency 5500MHz, is the line-of-sight (LOS) MPC. It arrives with about 0.8ns time difference from an azimuth angle of $120°$ at the two different antennas, which are spaced by about 25.5cm at $45°$. After beamforming for the LOS angles, it is clearly visible that more than one

maximum arises, which would lead to multiple LOS detections. The multiple wave detection problem is also shown in Fig. 5.

A simple way to avoid multiple MPC detection is to exclude short time intervals around the delays of already detected waves from the estimation process of other waves. For the span of the time intervals, the possible time difference of a wave arriving at different antenna locations should be considered. Hence, the time intervals depend on the spatial extent of the antenna array. The easiest way to define the time intervals is to simply compute the largest possible time of flight between any two antennas of the array. The time interval $\tau_{e,l}$ around the lth MPC, which is excluded from estimation for all other MPCs with $l' \neq l$, is given by

$$\tau_{e,l} = \left[\tau_l - \frac{d_{max}}{c}, \ \tau_l + \frac{d_{max}}{c} \right] \qquad (11)$$

where d_{max} is the largest distance between two antennas of the measurement array, and c is the speed of light, so that the estimation of parameter delay becomes

$$\hat{\tau}_l'' = \arg \max_\tau \left\{ \left| z(\tau, \hat{\phi}_l'; \underline{\hat{x}}_l(t; \underline{\hat{\theta}}')) \right| \right\} \Big|_{\tau \notin \tau_{e,l'}, \ l' \neq l}. \qquad (12)$$

V. Results

In order to demonstrate the performance of the proposed algorithm, real channel measurement data was analyzed. The measurements were taken with a vector network analyzer by IMST GmbH within the "why-less.com" project [11], [12]. The measuring system was set up in an office of about 5mx5m in size and 2.75m height with only very little inventory (see Fig. 4). It is assumed that the antenna used for the measurements is omnidirectional, meaning $f_m(\phi) = 1$ for $m = 1, \ldots, M$. A transmitter antenna was placed in a fixed position at 1.5m height, and the receiver antenna was moved along 30 parallel tracks at 1.5m height in the x-y plane, spaced 1cm apart, in 150 steps of 1cm, which makes a total of 4500 measured transfer functions with frequency resolution 6.25MHz.

For the demonstration of the results, UWB pulse transmission with different bandwidths is simulated for a 10x10 antenna array at several positions in the available measurement grid. Spacing between the antennas is chosen to be 2cm and the upper frequency band-edge of the transmitted pulse is set to 7500MHz. These settings meet the condition, that the distance between the antennas has to be half the wavelength matching the upper frequency band-edge to avoid ambiguities of the directions of arrival at all frequencies [13]. From previous measurement analysis in [12], [14] the number of paths L can be expected to be rather small, and is therefore set to 10.

For the illustration of the estimated delays and azimuths of the MPCs, the detected paths are plotted
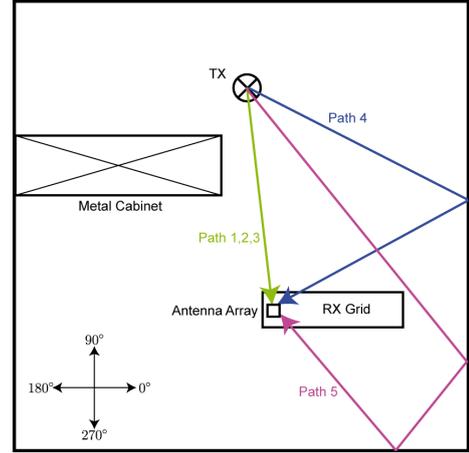

Fig. 4: Measurement environment and identified paths.

across the azimuth-delay scattering function arising from the received signals. Detected MPCs are plotted in greyscales according to their energy. The darker the dots, the stronger the energy of the wave. At first, it is again illustrated in Figs. 5 and 6 why the introduction of the time restriction interval is imperative. At large bandwidth 4000MHz without the time restriction interval, the LOS wave is detected multiple times, causing other strong waves not to be detected at all, while the result after introduction of the time restriction interval clearly shows the interval's help to avoid this problem.

Figs. 6 to 8 demonstrate the results gained with the proposed estimation procedure for bandwidths 4000MHz, 2000MHz and 500MHz, respectively. While with the lowest time resolution of 500MHz bandwidth none of the MPCs is detected more than once, for the higher time resolutions, despite the introduced time restriction interval, the LOS component and other strong waves are still detected more than once, though with little energy. On the other hand, at low time resolution MPCs are detected that at higher resolutions don't seem to actually be deterministic waves, as can also be seen in the azimuth-delay scattering function. Both these problems could be solved by choosing a more adequate number of paths L, though without exact knowledge of the number of received signal paths this could lead to undetected MPCs.

The five strongest MPCs that are detected with each of the four bandwidths, are the LOS wave from about $120°$ impinging at 10ns, followed by two waves from approximately the same direction that are probably reflections from floor and ceiling at 13ns and 16ns, a wave from $35°$ that is reflected by the wall to the right of the antenna array at 20ns, and a MPC from $325°$ originating from a reflection behind the array at 25ns (see Fig. 4).

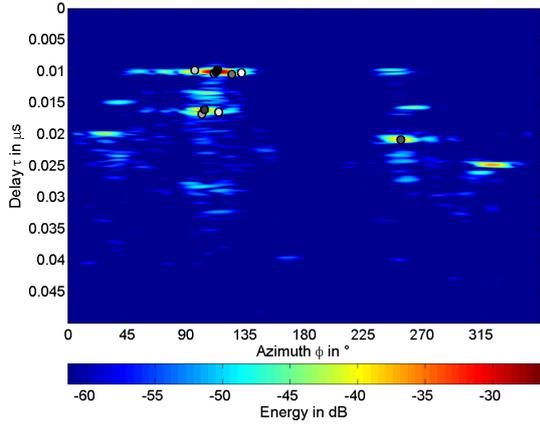To demonstrate the estimated complex amplitudes, the

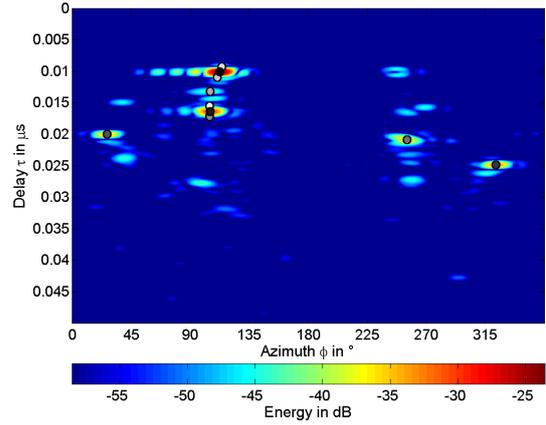Fig. 5: Multiple wave detection bandwidth 4000MHz.
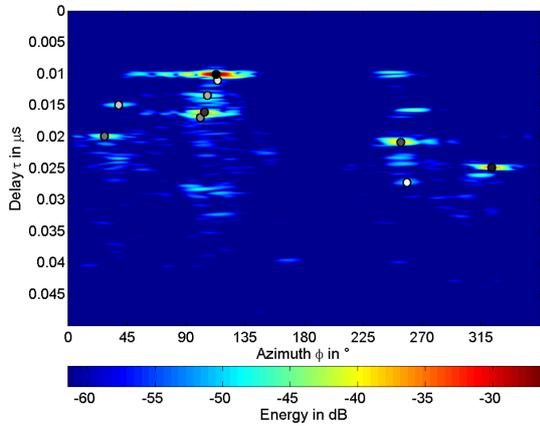

Fig. 7: Result for bandwidth 2000MHz.

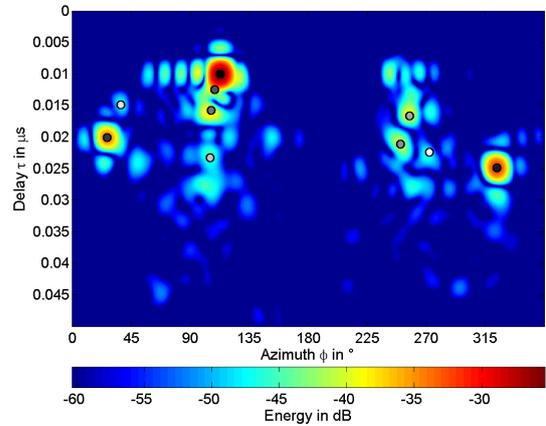Fig. 6: Result for bandwidth 4000MHz.

Fig. 8: Result for bandwidth 500MHz.

received signals for a specific antenna within the array are reconstructed with (2) and compared to the actually received signals. The results for different bandwidths are shown in Fig. 9. Even though the reconstructed signals are not completely accurate, for bandwidths 500MHz and 2000MHz, the received signal can be approximated quite well. Since the algorithm is designed to estimate deterministic MPCs, stochastic components that are present in the received signals are not visible in the reconstructed signals. At the highest time resolution the number of stochastic components missing in the reconstructed signal increases.

As path tracking possibilities of the obtained results are of interest, these are investigated in Figs. 10a-12a. For that purpose, propagation of the detected paths through the whole available measurement grid is visualized. The Figures show the magnitude of reconstructed signals versus delay, for antennas positioned side by side in a line parallel to the x-axis. Comparing these

plots to the magnitude-delay profiles of the measured signals at the same antennas in Figs. 10b-12b, it can be seen that, especially for large bandwidths, the MPCs can easily be tracked throughout the grid visually. The plots also clearly demonstrate the fact that the time difference it takes the waves to reach the different antennas within an array is not considered in the signal model. This negligence causes the propagation path of a wave to show discontinuities at the crossover between two antenna arrays. Such discontinuities are not present in the plots for the measured signals.

VI. CONCLUSIONS

A simple extension to the SAGE algorithm has been proposed to make it suitable for estimating delays, incident azimuths and complex amplitudes of deterministic MPCs in UWB channels. The algorithm has been applied to channel measurement data. Analysis of the results shows that the approach is capable of identifying
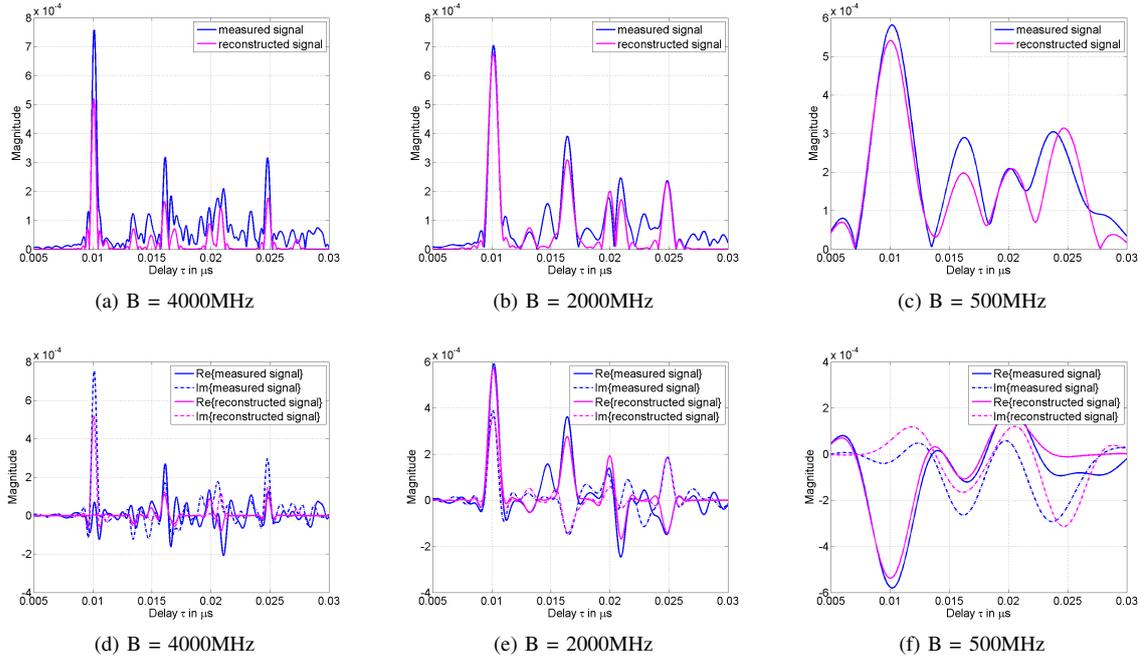
(a) B = 4000MHz   (b) B = 2000MHz   (c) B = 500MHz

(d) B = 4000MHz   (e) B = 2000MHz   (f) B = 500MHz

Fig. 9: Received and reconstructed signals.

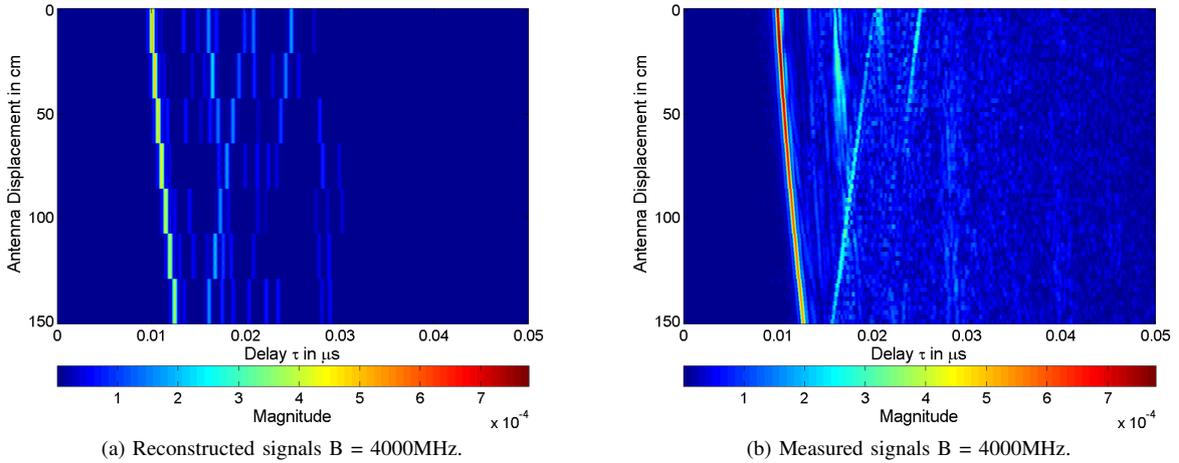(a) Reconstructed signals B = 4000MHz.   (b) Measured signals B = 4000MHz.

Fig. 10: Wave propagation through measurement grid.

individual impinging waves. It has been demonstrated that the channel can be approximated quite well by reconstruction of the received signals with the estimated wave parameters. An illustration of the detected MPCs propagating through several antenna arrays suggests path tracking potential.

The algorithm delivers satisfying results for all of the considered bandwidths, which leaves the ultimate choice of bandwidth open to meet other demands of particular applications.

REFERENCES

[1] S. Gezici, Z. Tian, G. Giannakis, H. Kobayashi, A. Molisch, H. Poor, and Z. Sahinoglu, "Localization via ultra-wideband radios: a look at positioning aspects for future sensor networks," *Signal Processing Magazine, IEEE*, vol. 22, no. 4, pp. 70–84, July 2005.

[2] R.-M. Cramer, R. Scholtz, and M. Win, "Evaluation of an ultra-wide-band propagation channel," *Antennas and Propagation, IEEE Transactions on*, vol. 50, no. 5, pp. 561–570, May 2002.

[3] T. Santos, J. Karedal, P. Almers, F. Tufvesson, and A. Molisch, "Scatterer detection by successive cancellation for UWB - method and experimental verification," in *Vehicular Technology*
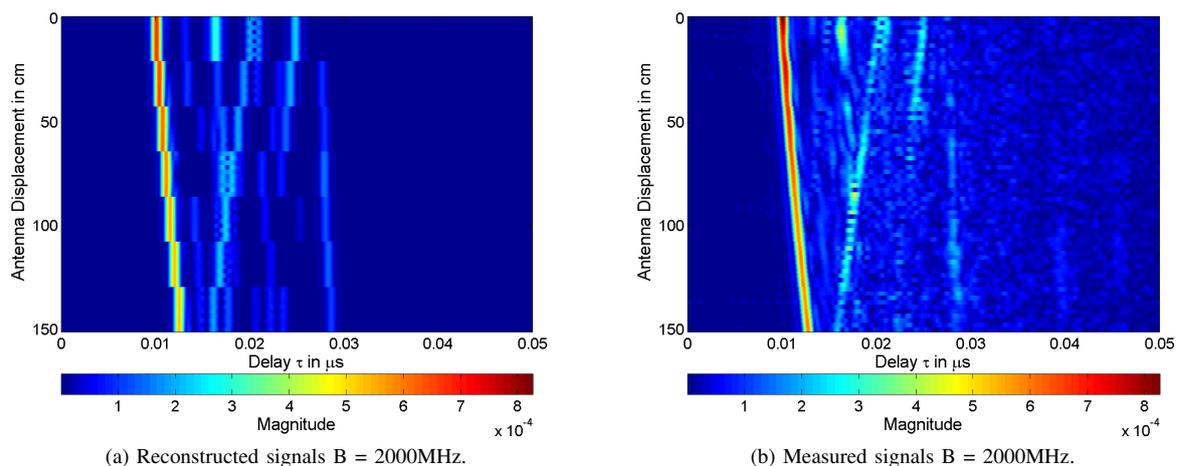
(a) Reconstructed signals B = 2000MHz.

(b) Measured signals B = 2000MHz.

Fig. 11: Wave propagation through measurement grid.

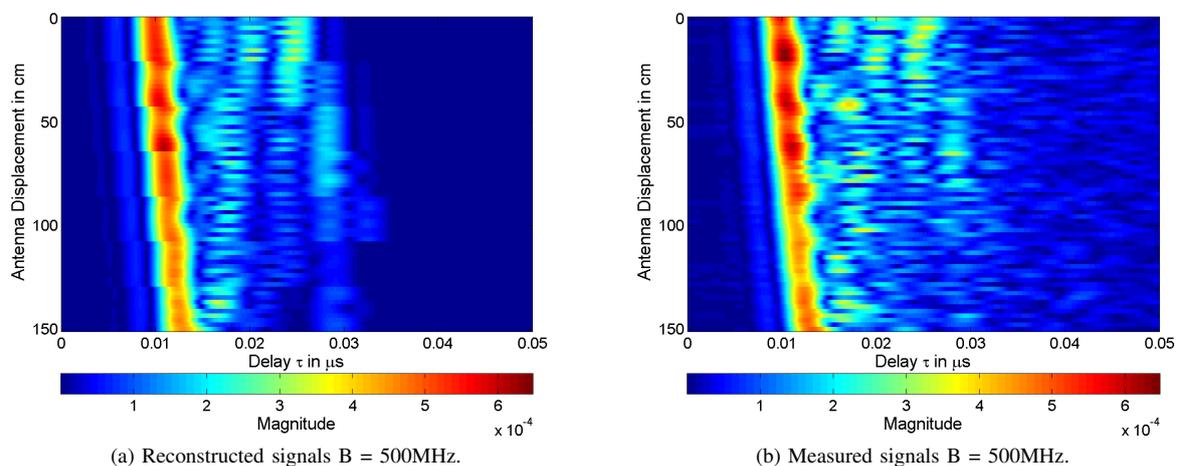(a) Reconstructed signals B = 500MHz.

(b) Measured signals B = 500MHz.

Fig. 12: Wave propagation through measurement grid.

Conference, 2008. VTC Spring 2008. IEEE, May 2008, pp. 445–449.

[4] K. Haneda and J.-I. Takada, "An application of SAGE algorithm for UWB propagation channel estimation," in *Ultra Wideband Systems and Technologies, 2003 IEEE Conference on*, Nov. 2003, pp. 483–487.

[5] K. Haneda and J. Takada, "High-resolution estimation of NLOS indoor MIMO channel with network analyzer based system," in *Personal, Indoor and Mobile Radio Communications, 2003. PIMRC 2003. 14th IEEE Proceedings on*, vol. 1, Sept. 2003, pp. 675–679 Vol.1.

[6] B. Fleury, D. Dahlhaus, R. Heddergott, and M. Tschudin, "Wideband angle of arrival estimation using the SAGE algorithm," in *Spread Spectrum Techniques and Applications Proceedings, 1996., IEEE 4th International Symposium on*, vol. 1, Sep 1996.

[7] M. Feder and E. Weinstein, "Parameter estimation of superimposed signals using the EM algorithm," *Acoustics, Speech and Signal Processing, IEEE Transactions on*, vol. 36, no. 4, pp. 477–489, Apr 1988.

[8] B. Fleury, M. Tschudin, R. Heddergott, D. Dahlhaus, and K. Ingeman Pedersen, "Channel parameter estimation in mobile radio environments using the SAGE algorithm," *Selected Areas in Communications, IEEE Journal on*, vol. 17, no. 3, pp. 434–450, Mar 1999.

[9] K. Pedersen, B. Fleury, and P. Mogensen, "High resolution of electromagnetic waves in time-varying radio channels," in *Personal, Indoor and Mobile Radio Communications, 1997. 'Waves of the Year 2000'. PIMRC '97., The 8th IEEE International Symposium on*, vol. 2, Sep 1997, pp. 650–654 vol.2.

[10] J. Fessler and A. Hero, "Space-alternating generalized expectation-maximization algorithm," *Signal Processing, IEEE Transactions on*, vol. 42, no. 10, pp. 2664–2677, Oct 1994.

[11] IMST GmbH, Carl-Friedrich-Gauss-Str. 2, 47475 Kamp-Lintfort, Germany, http://www.imst.com.

[12] "whyless.com − the open mobile access network,", IST-2000-25197, http://www.whyless.org, 2006.

[13] A. Molisch, "Ultra-wide-band propagation channels," *Proceedings of the IEEE*, vol. 97, no. 2, pp. 353–371, Feb. 2009.

[14] J. Kunisch and J. Pamp, "UWB radio channel modeling considerations," in *Proc. ICEAA 2003*, Turin, Sept. 2003.